

# Mechanical Properties of Cellularly Responsive Hydrogels and Their Experimental Determination

By April M. Kloxin, Christopher J. Kloxin, Christopher N. Bowman, and Kristi S. Anseth\*

Hydrogels are increasingly employed as multidimensional cell culture platforms often with a necessity that they respond to or control the cellular environment. Specifically, synthetic hydrogels, such as poly(ethylene glycol) (PEG)-based gels, are frequently utilized for probing the microenvironment's influence on cell function, as the gel properties can be precisely controlled in space and time. Synthetically tunable parameters, such as monomer structure and concentration, facilitate initial gel property control, while incorporation of responsive degradable units enables cell- and/or user-directed degradation. Such responsive gel systems are complex with dynamic changes occurring over multiple time-scales, and cells encapsulated in these synthetic hydrogels often experience and dictate local property changes profoundly different from those in the bulk material. Consequently, advances in bulk and local measurement techniques are needed to monitor property evolution quantitatively and understand its effect on cell function. Here, recent progress in cell-responsive PEG hydrogel synthesis and mechanical property characterization is reviewed.

cultured in 3D, in contrast to those cultured in 2D, exhibit cellular responses similar to those observed in vivo.<sup>[1]</sup> As a result, tissue engineers and biologists are often faced with the need for a more physiologically relevant 3D culture environment, which has led to growing interest in hydrogels as a means of creating custom 3D microenvironments with highly controlled biochemical and biophysical properties. Hydrogels based on native proteins (e.g., Matrigel, collagen) have been explored extensively for applications in 3D tissue culture and regenerative medicine. Protein gels provide a plethora of biochemical cues and recapitulate numerous aspects of the natural ECM, but unfortunately, they also pose difficulties for precisely controlled cell culture. Protein-based gels are often complex, variable, and ill-defined compositionally, making the responses of cells embedded within them difficult to deconvolute and

## 1. Introduction

Physiological processes are generally guided by interactions that occur between cells and their local tissue environment, i.e., the extracellular matrix (ECM). Recent research has demonstrated that this interrelationship between cells and their local environments stretches far beyond native interactions, such as cell integrin binding to ECM and cellular response to soluble factors, and plays a significant role in dictating cellular behavior in culture as well. More specifically, there is a growing, insightful body of literature demonstrating that significant differences in cell phenotype arise when cells are cultured on petri dishes or material surfaces with unnaturally high stiffness, polarity, and surface to volume ratio as compared to their native tissue microenvironment.<sup>[1–3]</sup> For example, mammary epithelial cells

In contrast, typical synthetic hydrogels promote engineering of well-defined material mechanics and structures, but often lack biological epitopes to interact with soluble or cell-surface proteins. Thus, synthetic hydrogels often provide little more than a blank slate that permits, but does not control, cellular function in the absence of contextual instructions. Consequently, the need for matrices that combine the benefits of natural and synthetic hydrogels has become more apparent, along with the need to identify the necessary and sufficient time-dependent biophysical and biochemical signals to incorporate within these synthetic extracellular matrix analogs. To complicate the situation further, the native ECM is far from static, so hydrogel ECM mimics must also have dynamically tunable properties that direct and respond temporally to complex cellular behavior.

Towards the goal of developing ECM mimics, especially cellularly responsive hydrogel systems, several approaches have been taken. Self-assembled peptide systems are formed under physiological conditions (i.e., temperature and pH) and have been shown to direct neural progenitor cell differentiation<sup>[4]</sup> and permit human mesenchymal stem cell (hMSC) chondrogenesis in 3D.<sup>[5]</sup> In addition, self-assembled artificial protein systems promoted endothelial cell attachment and proliferation in 2D towards the development of improved vascular grafts.<sup>[6]</sup> These gels provide elegant approaches to engineer the presentation of selected biological epitopes and capture many aspects of the architecture/fibrillar structure of native ECM proteins.

[\*] Dr. A. M. Kloxin, Dr. C. J. Kloxin,  
Prof. C. N. Bowman, Prof. K. S. Anseth  
Department of Chemical and Biological Engineering  
University of Colorado  
424 UCB ECCH 111, Boulder, CO 80309 (USA)  
E-mail: Kristi.Anseth@colorado.edu  
Dr. A. M. Kloxin, Prof. K. S. Anseth  
Howard Hughes Medical Institute  
University of Colorado  
Boulder, CO 80309 (USA)

DOI: 10.1002/adma.200904179

While these materials fill an important niche, the nature of the physical crosslinking limits their mechanical properties, which often necessitates that they cannot be placed under physiologically relevant loads. Thus, self-assembled systems have a limited range over which one can tune the network elasticity and evaluate the influence of mechanotransduction on cell behavior. As a result, covalently crosslinked gels, including artificial protein-based<sup>[7]</sup> and synthetic polymer-based<sup>[8,9]</sup> hydrogels, provide several distinct benefits, including tailored presentation of biological epitopes, controlled gel formation and degradation, and robust mechanical properties that allow gel loading and mechanotransduction. One class of covalently crosslinked hydrogels are based on poly(ethylene glycol) (PEG). PEG is widely used in human medicine and resists protein adsorption, imparting unique nonfouling properties. The crosslinking of PEG through one of a variety of methodologies provides a basis from which to manipulate gel material properties, whereas chemical functionalization of PEG provides a means to systematically introduce biological signals. These biological signals include ligands, which allow one to determine the relationship between specific biological material interactions and cell function, as well as cell-cleavable sequences, which promote local cellular remodeling of their material environment. Functionalized PEG gels can be formed via either chain or step growth polymerization (Figure 1), depending on the functional, polymerizable moieties that are incorporated pendant to the PEG molecules. These types of PEG gel systems for 2D and 3D cell culture and strategies to characterize their unique mechanical properties are the focus of this review.

## 2. PEG-Based Hydrogel Formation and Characteristics

A common and robust approach to synthesize PEG hydrogels is the photoinitiated chain polymerization of macromolecular PEG chains modified on either end with acrylate or methacrylate moieties.<sup>[10]</sup> This photoinitiated reaction enables hydrogel formation under physiological and cytocompatible conditions,<sup>[11]</sup> while also affording temporal and spatial control of the network evolution.<sup>[12]</sup> The resulting network structure consists of a distribution in the crosslinking density with long poly(meth)acrylate kinetic chains crosslinked by PEG (Figure 1).<sup>[13]</sup> It is important to note that the macromolecular nature of the crosslinking molecule, which is often homopolymerized in aqueous solutions, renders many classical theories insufficient for hydrogel characterization. For example, the Flory–Rehner theory<sup>[14]</sup> requires knowledge of the molecular weight of the network polymer chains in the absence of crosslinks ( $\bar{M}_n$ ).  $\bar{M}_n$  is generally unknown for these in-situ-formed gels and only measurable following degradation. More importantly, the nature of the macromolecular monomers themselves leads to crosslinks that are not point junctions, dramatically influencing the calculation of the average molecular weight between crosslinks ( $\bar{M}_c$ ). Further, network imperfections, such as cycles and dangling chain ends, are highly prevalent, form to vastly different extents depending on the reaction conditions, and make calculation of related network properties difficult and often inconsistent with experimental observations. Towards the creation of more biomimetic and



**Christopher N. Bowman** is a Patten Professor in the Department of Chemical and Biological Engineering and a Clinical Professor of Restorative Dentistry at the University of Colorado. He received his B.S. and Ph.D. in Chemical Engineering from Purdue University in 1988 and 1991, respectively. He works in the broad areas of polymerization reaction

engineering, polymer chemistry, photopolymerizations, and biomaterials. He serves as co-director of the NSF/Industry Cooperative Research Center for Fundamentals and Applications of Photopolymerizations.



**Kristi S. Anseth** is a Howard Hughes Medical Institute Investigator and Distinguished Professor of Chemical and Biological Engineering at the University of Colorado. She received her B.S. in Chemical Engineering from Purdue University in 1992 and her Ph.D. in Chemical Engineering from the University of Colorado in 1994. She is an elected

member of the National Academy of Engineering and the Institute of Medicine.

responsive hydrogel systems, adhesive ligands and proteolytic degradation sites are readily incorporated by copolymerization of the crosslinking macromers with acrylate functionalized peptides,<sup>[15]</sup> permitting cells to interact with and/or remodel their microenvironments. However, the nature of the chain polymerization and its associated formation of a carbon–carbon backbone polymer necessitates that cleavable groups for gel degradation must be introduced within the crosslinks. The classically observed polydispersity in the kinetic chain length and crosslinking density is both an advantage (e.g., rapid and robust gel formation) and disadvantage (e.g., non-uniform degradation products and heterogeneous nanoscale structure) of this type of gel system.

As an alternative to the widely used PEG-di(meth)acrylate systems, step growth polymerizations have emerged. PEG gels are readily synthesized by the reaction of comonomer solutions containing complementary reactive groups. The resulting hydrogels possess more homogeneous network structures (Figure 1), which often lead to superior mechanics when compared to chain growth networks of similar crosslink density.<sup>[16]</sup> Such hydrogels have been synthesized using base-catalyzed Michael-type addition reactions between thiols and conjugated unsaturated

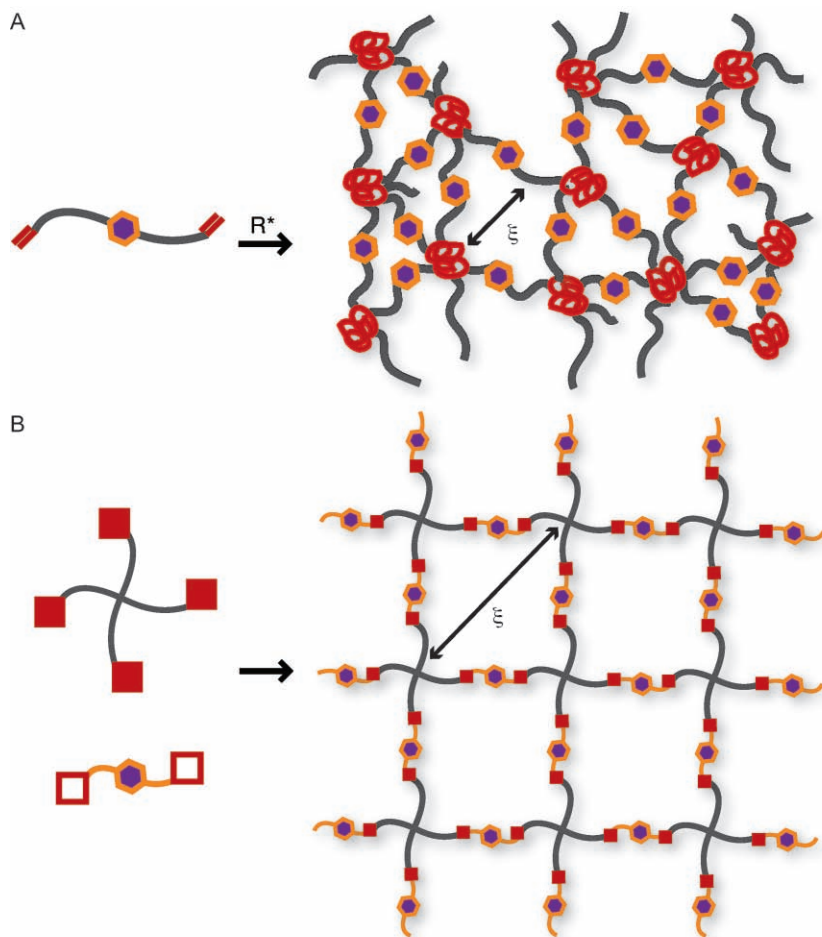


**Figure 1. PEG hydrogels.** Two common methods of forming PEG-based hydrogels are chain growth and step growth polymerization of multifunctional PEG monomers. A) PEG di(meth)acrylate monomers (left, gray PEG chain with red (meth)acrylate end groups; PEGDMA) are polymerized by free radical chain polymerization, forming coiled poly(methacrylate) chains (right, red coils) connected by PEG (gray linkers). Here, the molecular mesh size of the network ( $\xi$ ) is dictated by the length of the PEG chain and the concentration of PEGDMA in the gel-forming solution. In addition, the crosslinking density of the network ( $\rho_c$ ) is controlled by the concentration of PEGDMA, dictating the resultant gel modulus, equilibrium water content, and solute diffusivity. Degradation is easily introduced within these gels by incorporation of a degradable moiety (purple and orange hexagon; water, enzyme, or light degradable group) within the PEGDMA crosslinking monomer. B) Multifunctional PEG monomers (gray 4-arm PEG with red box reactive end group) are reacted stoichiometrically with degradable linkers (orange linker with open red box reactive end groups and purple hexagon degradable group) to form nearly perfect networks by step growth polymerization. The reactive end groups may include acrylates and thiols polymerized by base-catalyzed Michael-type reaction, norbornenes and thiols by free radical initiation, and azide and alkynes by copper-based or copper-free click reaction. Here, the mesh size is again dictated by the length of the PEG chain, whereas the crosslinking density is dictated by the length and concentration of the PEG crosslinker.

functional groups,<sup>[17]</sup> radical-mediated thiol-ene photopolymerizations,<sup>[18]</sup> and even copper-free Huisgen cycloaddition ('click' reaction) between azide and alkyne-functionalized PEG precursors.<sup>[19]</sup> For the thiol-ene and Michael addition, the step growth polymerization provides a simple strategy for incorporating proteolytically degradable peptides through the inclusion of cysteine, which readily copolymerizes in these approaches, on one or both

ends of targeted peptide sequences. Hydrogels that promote cell spreading and migration in a fashion similar to natural biomaterials have been synthesized with this approach.<sup>[20–23]</sup>

While these covalently crosslinked gels provide many benefits from an applications perspective, especially their enhanced mechanical properties, the covalent interactions also impart many complications. First, protein diffusion is hindered. Long mass transfer time-scales influence the delivery and distribution of important cytokines or other growth factors to encapsulated cells, as well as the ability of cells to secrete and elaborate their own extracellular matrix, which is important for tissue engineering processes. For example, transforming growth factor- $\beta_1$  (TGF- $\beta_1$ ) delivery to encapsulated hMSCs enhances chondrogenic differentiation,<sup>[24]</sup> and diffusion of growth factors such as this one can be hindered in a densely crosslinked gel or in a thick gel construct.<sup>[25]</sup> In addition, encapsulated hMSCs that differentiate into chondrocytes secrete collagen type II and glycosaminoglycans; elaboration of these secreted proteins within the gel construct has been shown to be largely dependent on gel crosslinking density and degradation rate, affecting the mechanical properties of the regenerated tissue.<sup>[26]</sup> Second, the molecular nature of the crosslinking density and related mesh size renders cells ( $\sim 10 \mu\text{m}$  diameter) effectively immobile. As a result, degradation of the material environment must be incorporated and controlled to enable cell migration for studying cancer metastasis,<sup>[27,28]</sup> angiogenesis,<sup>[29,30]</sup> and wound healing<sup>[31]</sup> and to facilitate cell–cell interactions for controlling cell function and directing tissue morphogenesis,<sup>[32,33]</sup> amongst other applications. While this degradation can mimic certain aspects of natural cell migration and ECM remodeling, by allowing cell-dictated degradation through the incorporation of enzymatically degradable sequences,<sup>[20]</sup> deciding which degradable sequences to use and knowing how cells are degrading their local environment is a complex problem. Enzymatically degradable sequences utilized in PEG-based hydrogels include GGLGPAGGK degraded by collagenase;<sup>[34]</sup> AAAAAAAAAAK,<sup>[34]</sup> AAPVR, and AAP(Nva)<sup>[35,36]</sup> degraded by elastase; and GPQGIWGQ, GPQGIAGQ, and GPQGILGQ, which are degraded by collagenase and various matrix metalloproteinases (MMPs), such as MMP-1, -2, -3, -7, -8, and -9.<sup>[18,37–38]</sup> Cell degradation of hydrogels containing these sequences is cell-type-dependent, and because of this feature, tailoring the gel degradation properties to a particular cellular system is still largely empirical.

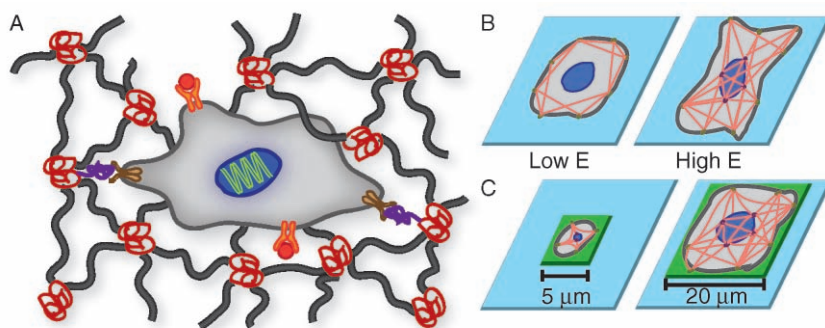


**Figure 2. Complexities of the cell environment and cellular response to substrate mechanics.**

A) Cells respond to multiple signals within their microenvironment. Studies often focus on the effect of soluble factors (integrin-bound red circles) and genetics (green DNA strands in the nucleus) on cell function while less attention is given to the structure and mechanics of the gel with which the cell is interacting, where the cell binds to ligands tethered to its microenvironment (purple coils) and pulls on the surrounding structure. To address this issue, 2D studies of cell–gel interactions have been undertaken. B) Cells cultured on low modulus substrates exhibit a diffuse cytoskeleton (orange actin fibers), whereas cells cultured on high modulus substrates exhibit a dense actin cytoskeleton, leading to different differentiation pathways for hMSCs, e.g., neurogenic ( $\sim 1$  kPa), myogenic ( $\sim 10$  kPa), and osteogenic ( $>25$  kPa) pathways, through mechanotransduction.<sup>[40]</sup> C) Similarly, cell shape has been shown to influence cytoskeletal organization and cell fate, where cells cultured on small islands of fibronectin (green) undergo apoptosis (left) while cells on larger islands ( $>10$   $\mu\text{m}$ ) undergo proliferation (right).<sup>[42]</sup>

### 3. Interplay Between Gel Mechanics and Cell Function

To date, experiments with cell-laden hydrogel constructs have contributed to our understanding of stem cell differentiation, tissue morphogenesis, and pathophysiology. However, the field has been largely dominated by the paradigm that the primary regulators of cell function are genetic and chemical factors, and the critical, dynamic interplay between ECM ligands and cell surface receptors as well as cytoskeletal organization (Figure 2A) are often overshadowed. Seminal 2D experiments emphasized the relationship between cell function and mechanical signals in the cellular microenvironment and implicated integrin binding, focal adhesion formation, and the actin cytoskeleton as transducers of these signals.<sup>[39]</sup> Specifically, Discher and his colleagues demonstrated that the differentiation of hMSCs is dependent on the mechanical stiffness of the 2D culture platform (Figure 2B).<sup>[40,41]</sup> Further, Ingber and his colleagues have shown that the degree to which a cell is mechanically extended by adhesive ligands on a 2D scaffold can dictate relative growth and apoptosis rates (Figure 2C).<sup>[42–45]</sup>

Beyond these 2D studies, Bryant et al. encapsulated chondrocytes in PEG gels and examined how cells responded to dynamic loading.<sup>[46]</sup> An interesting aspect of this work points to further complexities in the cell

microenvironment. Namely, cells respond in a nonhomogeneous fashion to macroscopic gel deformation/strains. Chondrocytes encapsulated within nondegradable PEG gels were cyclically compressed with different strain percents, and the resultant cell deformation was observed with confocal microscopy (Figure 3). While gel deformation on the macroscopic scale was uniform, microscopic cell deformation varied from cell to cell and nonlinearly with applied strain. These studies indicate that, not only is the gel structure heterogeneous on the nanoscale, but cellular response to gel structure and mechanics is heterogeneous due to variations within the cell population and life cycle. Understanding and controlling cellular response to mechanical forces in 3D is complex, as non-uniform gel properties and heterogeneous cell populations can lead to non-uniform cellular responses to stimuli,<sup>[47]</sup> and introducing degradability within the gel further complicates this analysis.

Despite the significance of these 2D and 3D examples, they only probe the cellular response in static, nondegrading material systems. An important aspect of numerous

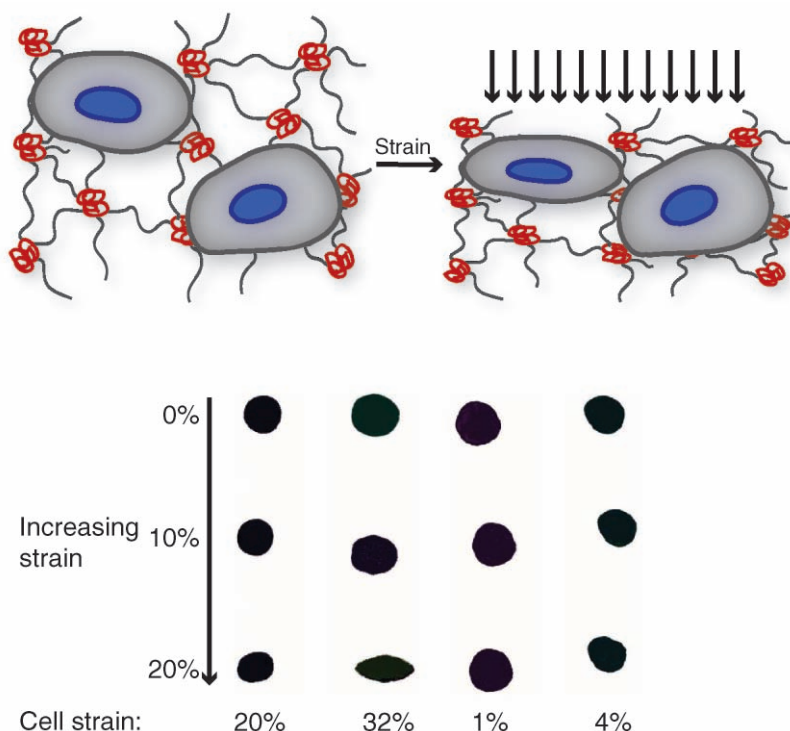


**Figure 3. Cell response to mechanical stimulation in 3D.** Cells encapsulated within a gel respond to applied mechanical strain non-uniformly (top). Specifically, individual chondrocytes show varying degrees of deformation in response to increasing strain, as observed with confocal microscopy, where cells in gels under 20% strain deform between 1 and 32%. While the gel structure is heterogeneous on the nanoscale, the cellular response to gel structure and mechanics is heterogeneous on the micro and macroscale. Reproduced with permission.<sup>[46]</sup>

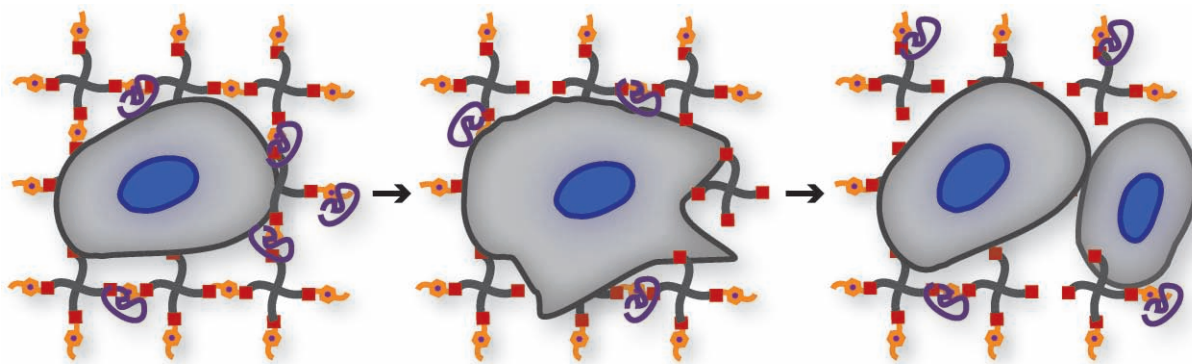


**Figure 4. Dynamic modification of the microenvironment.** Cells encapsulated within PEG gels initially exhibit a rounded morphology (left). Within an enzymatically degradable gel, cell-secreted enzymes (purple coils) begin to breakdown the local matrix surrounding the cell, enabling cell spreading and movement (middle) and subsequently cell division (right). Monitoring these dynamic and local changes in gel mechanics in response to cell degradation is challenging.

other ECM-hydrogel mimics is that they degrade in response to cell-secreted proteases. This process is often local, and typically observed by changes in cell morphology and movement (Figure 4). For example, cells encapsulated within PEG gels initially exhibit a rounded morphology. To promote spreading and movement at different points in their life cycle, cells secrete enzymes to degrade the local matrix, initially extend small processes to probe the surrounding environment, and subsequently migrate and/or divide.<sup>[18,29]</sup> However, understanding the mechanisms by which cells are receiving information from their material microenvironment combined with how the material is responding to cellularly dictated changes becomes increasingly complex. Monitoring these dynamic processes is important to answer biologically important questions, as well as improve on the design of hydrogel carriers for cell delivery and tissue engineering.

## 4. Real-Time Monitoring

### 4.1. Cell Motility and Function

Researchers routinely employ real-time cell tracking to monitor changes in cell morphology and quantify the speed and persistence of migrating cells.<sup>[31,48]</sup> Migration is particularly important to characterize in 3D, as the mechanism is quite different for cells migrating on a surface as compared to those embedded in an ECM-like environment. To provide molecular-level information, reporter-based systems and intracellular mechanical measurement techniques have been developed to elucidate real-time changes in cell function and cytoskeletal organization. In the reporter-based systems, gene and protein expression are linked with the production and localization of reporter proteins, such as green fluorescent protein (GFP), allowing non-invasive monitoring of changes in cellular processes via fluorescent imaging.<sup>[49,50]</sup> For example, cells can be engineered to produce GFP-labeled proteins, such as  $\beta$ -actin labeled with GFP for in situ monitoring of actin fiber formation and cytoskeletal organization,<sup>[51]</sup> and

fluorescence resonance energy transfer (FRET)-labeled proteins, such as protease-sensitive linkers labeled with cyan fluorescent protein (CFP) paired with yellow fluorescent protein (YFP) for measuring caspase activity during apoptosis.<sup>[52]</sup> More specific to capturing microenvironmental remodeling, MMP localization by engineering cancer cells (HT1080s) to express GFP-labeled MMP-1 and cell-dictated restructuring of collagen gels have been observed with dynamic multimodal microscopy.<sup>[53]</sup>

In addition, microscopic changes in intracellular mechanics are monitored with micromechanical measurements, such as microrheology and atomic force microscopy (AFM).<sup>[54]</sup> For example, Baker et al. recently used microrheology to observe that prostate cancer cells show increased intracellular creep compliance, a measure of cytoplasmic modulus, with increased matrix modulus in 3D culture, whereas no correlation was observed in 2D culture, which may account for phenotypical differences observed in cancer cells when cultured in 2D versus 3D.<sup>[55]</sup> Forces exerted by the cell on their microenvironment are monitored using particle tracking, specifically traction force microscopy (TFM), where it was recently observed that fibroblasts migrating on poly(acrylamide) surfaces exert forces in 3D.<sup>[56]</sup> Cell-cell mechanical communication has also been examined with TFM, where transmittance of traction stresses between cells was found to vary with substrate modulus.<sup>[57]</sup>

Many tools for studying dynamic cell functions are currently available, including cell-reporter-based systems, microrheology, AFM, and TFM, techniques covered in detail in several other reviews.<sup>[49–50,54,58]</sup> Taken together, a substantial toolbox for monitoring cellular processes and mechanics exists and continues to grow with fluorescent-probe and micromechanical measurement systems.

### 4.2. Localized Gel Degradation

While real-time techniques for measuring cellular processes have been developed and successfully applied, fewer methods have emerged for in situ characterization of changes in the material microenvironment during cellularly dictated degradation

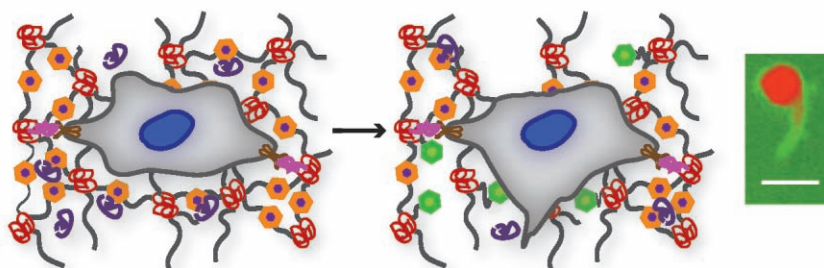


**Figure 5. Detection of local gel degradation.** FRET-based linkers within gels provide a means to locally detect cell-directed gel degradation. As the cell degrades crosslinks within the gel (left, orange hexagon degradable blocks cleaved by purple cell secreted enzymes), increased fluorescence is observed (middle, green hexagon fluorescent groups). Cells can subsequently extend processes and move within the degraded gel, leaving tracks of increased fluorescence (right, scale bar 20  $\mu\text{m}$ ). Reproduced with permission.<sup>[59]</sup> Copyright 2007, El Sevier.

and remodeling. One qualitative approach to detect local degradation in gel systems uses the incorporation of a FRET-based linker within the gel-forming macromers. For example, Lee et al. incorporated a FRET-based dye system into a collagenase degradable linker within a PEG-based gel.<sup>[59]</sup> Upon local gel degradation by encapsulated fibroblasts, increased fluorescence was observed, allowing visualization of the degradation tracks generated by migrating cells (Figure 5). Simultaneously, Kong et al. developed a FRET-based reporter system for monitoring polymer chain conformation as a function of gel crosslinking density in alginate-based gels towards real-time measurement of gel degradation.<sup>[60]</sup> While these techniques are each useful for monitoring local changes in the network structure, complementary techniques are needed for measuring local material properties in real-time and enabling quantification or semiquantification of properties, such as modulus and crosslinking density, to understand more completely how they are evolving during local, cell-dictated degradation.

## 5. Importance of Understanding Gel Crosslinking Density for 3D Cell Culture

From the perspective of the cellular environment, the important biophysical and biochemical properties of hydrogels include, but are not limited to, i) physiological water content for transport and cell survival, ii) tissue-like elasticity for mechanotransduction, iii) diffusivity of important cell-secreted molecules and/or delivery of cytokines and morphogens from the culture media, iv) ligand presentation for promoting cell adhesion and function, and v) degradability for matrix remodeling and ECM elaboration. All of these factors depend on and are strongly coupled through the crosslinking density of the network. Because of the complex changes that occur in both the structure and chemistry of crosslinked hydrogels during degradation, rheological characterization is an extremely powerful tool to characterize the gel properties, specifically modulus, and through it, crosslinking density. Initial and time-dependent properties are readily measured

in both the bulk and local gel. Here, bulk property measurements will be reviewed first, and beyond allowing characterization of the initial properties of gels, these measurements often enable mechanistic understanding of changes occurring in gels that degrade homogeneously. Subsequently, the importance of local property measurements and the development of techniques for quantitatively measuring them, including AFM and microrheology, will be addressed. Such techniques are quite useful for characterizing gels that are undergoing cellularly dictated degradation and remodeling, which can lead to local microenvironmental properties that are significantly different from the bulk.

## 6. Bulk Gel Mechanical Measurements

The network architecture of a hydrogel is responsible for holding cells in place, as a scaffold, while also providing diffusional access for cell-signaling cues, nutrients, and other moieties introduced into the cell culture environment. The key structural parameter dictating the material modulus, as well as the diffusional characteristics, is the network crosslinking density. Many of the techniques employed to characterize nonhydrated, neat polymer networks, such as mid-IR spectroscopy and differential scanning calorimetry, are problematic when applied to hydrogels owing to their large water content (typically >90%). Whereas small angle neutron and light scattering have been used to characterize the network architecture, dynamic mechanical analysis (DMA) is a facile method for characterizing the bulk mechanical properties and the underlying crosslink density of the hydrogel. In particular, rheometry (i.e., defined here as shear-mode DMA) is a convenient method for in situ fabrication and characterization of hydrogels, while reducing practical experimental difficulties such as sample clamping and dehydration.

Amongst the more successful theories relating bulk properties to the underlying microscopic structure of a material is rubber elasticity theory, roughly stating that the rubbery modulus scales with the crosslinking density and the temperature ( $E \sim \rho T$ ).<sup>[14,61–65]</sup> The basic assumptions underlying rubber elasticity theory are that crosslinked polymer strands are connected at points and are represented by a Gaussian distribution. The exact form of this relationship depends on a number of factors, including the material's compressibility (Poisson's ratio) and anisotropy, the network architecture model (i.e., the affine or phantom model), network defects (i.e., loops and dangling ends), the inclusion of entanglements, solvent effects (i.e., network swelling), and the extent of deformation.<sup>[66]</sup> Moreover, swelling of a network has a substantial effect on the modulus and depends greatly on the concentration and solvent quality. Neglect of these various considerations can result in a significant over- or under-estimation of the modulus from the ideal classical form (i.e.,  $G = \rho_x k_B T$ , where  $G$  is the rubbery shear modulus, which is related to  $E$  via the Poisson's ratio, and  $\rho_x$  is the number of crosslinking strands per volume), but the scaling relationship remains intact. To utilize rubber elasticity

theory with rheometry, sinusoidal linear deformation measurements are made in the low frequency ( $\omega$ ), rubbery regime to capture the shear modulus of the network ( $G = \lim_{\omega \rightarrow 0} G'(\omega)$ , where  $G'$  is the elastic or storage shear modulus).<sup>[67]</sup> Thus, rheological measurements of  $G'$  must be nearly independent of frequency and further must be independent of the applied strain (i.e., in the linear viscoelastic (LVE) regime) to be directly interpreted using rubber elasticity theory. The hydrogel's response to low frequency sinusoidal deformation reflects crosslinked hydrophilic chains surrounded by water. Nanoscale heterogeneities observed in some hydrogels<sup>[13]</sup> are lost in bulk rheometric measurement interpreted using mean field-based rubber elasticity theory. For example, the polyacrylate coils crosslinking PEG (Figure 1A) become coarse-grained multifunctional crosslinking units connected via PEG crosslinking segments. This outcome is the same that would be observed for bulk measurements in homogeneous hydrogels.

With these considerations addressed, several researchers have employed rheometry to monitor gelation kinetics while also characterizing the liquid-to-solid transition in hydrogels (Figure 6).<sup>[18,38]</sup> It should be noted that this transition is frequently and incorrectly deemed the point where an incipient gel forms, or the so-called gel-point. Rather, the gel-point is typically marked by the Winter–Chambon criterion, where the elastic and viscous modulus scale identically with frequency ( $G' \sim G'' \sim \omega^\lambda$ ),<sup>[68,69]</sup> nevertheless, the gel-point tends to be in the vicinity of the liquid-to-solid transition ( $G'-G''$  crossover).<sup>[70]</sup>

Beyond gel formation, rheometry and other DMA techniques have been used to characterize the modulus of gel samples formed with different crosslinking densities. For example, numerous studies have used hydrogel systems of varying

crosslinking density to evaluate the static elastic modulus of gels and then used these gels for 2D cell culture towards elucidating mechanotransduction effects on cell properties.<sup>[40,71–76]</sup> Emerging areas of interest include translating this understanding to cells encapsulated in systems with defined elasticity, where focal adhesions, cell morphology, and polarity can be quite different than in 2D. Beyond tailoring the initial properties of the gel, hydrogel systems have recently been developed to allow the formation of cell substrates that have a triggered change in elasticity at any point in time. For instance, using photopolymerization, Hahn et al. have increased the modulus of PEG gels in situ by the selective addition of short crosslinking molecules within an existing gel, increasing the crosslinking density in space and time.<sup>[12]</sup> Khetan et al. have photocoupled peptide crosslinks within covalently crosslinked hyaluronic acid gels, temporally increasing the local crosslinking density and controlling cell morphology in 3D,<sup>[77]</sup> and Nowatski et al. have increased the crosslinking density of DNA-based gels via photocoupling in 2D.<sup>[78]</sup> Gel modulus also has been decreased in situ by photocleavage of gel crosslinks with controlled irradiation, controlling cell migration and morphology in 2D<sup>[48]</sup> and 3D.<sup>[79]</sup> Such probing of cell responses to dynamic changes in their environment may prove quite useful in expanding the current understanding of the role of the material environment in focal adhesion formation, migration, and even differentiation.

While bulk measurements provide a global picture of the 3D cell culture environment, there are several questions that still remain about how cells react to local spatial variation or how far into the material a cell is able to sense property changes. As these questions are crucial for understanding many of the basic questions about how cells are responding to their material microenvironment, new methods for probing the local mechanical properties must be developed. These methods must have a spatial resolution smaller than the size-scale of a cell to determine local variation in the mechanical properties. Among these methods are AFM and tracer particle microrheology.

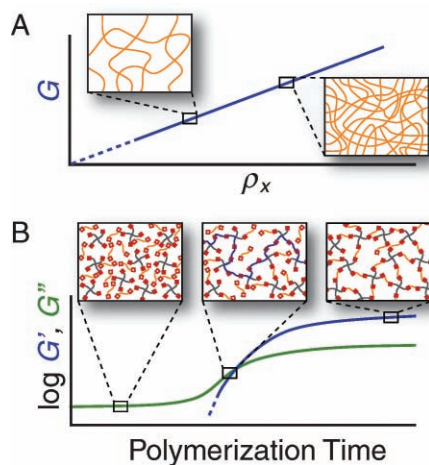


**Figure 6.** Bulk property measurement with rheometry. A) As the modulus is a function of crosslinking density, B) the polymerization progression can be monitored utilizing oscillatory bulk rheometry. Initially monomeric and oligomeric species yield a viscous response to oscillatory deformation, where the viscous modulus ( $G''$ ) dominates the viscoelastic spectrum. With polymerization, the formation of the incipient gel occurs (shown in the second inset of panel B), defining the gel point of the material. The gel point is typically in the vicinity of, but rarely at, the elastic and viscous moduli crossover. At the end of the polymerization, the hydrogel network becomes fully formed with the elastic modulus ( $G'$ ) dominating the viscoelastic spectrum.

## 7. Atomic Force Microscopy (AFM)

The growing recognition of the important role of the microenvironmental modulus in dictating cell functions such as differentiation,<sup>[40,80–81]</sup> migration,<sup>[82]</sup> and fate<sup>[83]</sup> has led to extensive use of AFM for determining local gel and cell mechanical properties.<sup>[84]</sup> To determine local surface modulus, the AFM is used in contact mode, where the probe measures force versus distance at a specific point on the gel surface (Figure 7A). The force versus distance data acquired from lowering and subsequently retracting the probe to and from the surface is converted into the surface modulus with the spring constant for the probe and by selection of a model for elasticity and Poisson's ratio ( $\nu$ ) for the material of interest.<sup>[85,86]</sup> The spring constant is easily determined using a standard substrate. The Hertz model is often used for describing hydrogels, and using it, good agreement between bulk and surface measurements of gels has been shown.<sup>[78]</sup> Last, Poisson's ratio, which can vary for different hydrogel types, has recently been shown to differ

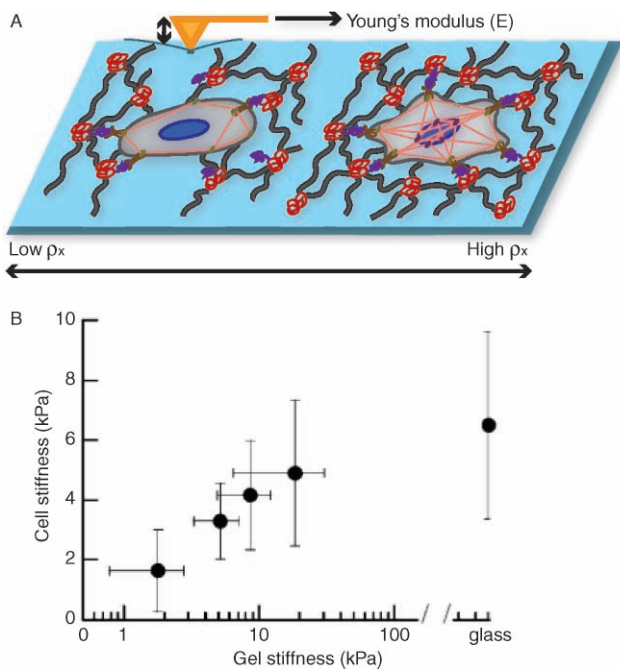


**Figure 7. AFM for local surface measurement of gel modulus and crosslinking density.** A) Cells on substrates of different crosslinking densities exhibit different cytoskeletal organization and moduli. A cell on a highly crosslinked gel (right) has a cytoskeleton dense with actin fibers (orange) and focal adhesions (green), pulling on the network through integrin–ligand binding (brown and purple) and responding to the elasticity of the substrate, whereas a cell on a less crosslinked substrate has a diffuse cytoskeleton (left). With AFM, the modulus, and thus crosslinking density, of the underlying gel as well as the modulus of the cell's cytoskeleton can be measured by controlled indentation of the sample surface during 2D cell culture (top) to explore this interplay between gel structure and cell function. B) A correlation between substrate stiffness and cell stiffness was observed with AFM measurements of fibroblasts cultured on polyacrylamide gels of varying crosslinking density. Reproduced with permission.<sup>[89]</sup> Copyright 2007, Cell Press.

for a hydrogel surface measured with AFM in comparison to bulk hydrogel measurements, where  $\nu$  is 0.2 for a gel surface, which does not have adequate time to relax or drain during the nanoscale perturbation with an AFM probe,<sup>[87]</sup> and is 0.45–0.5 for a bulk PEG gel.<sup>[88]</sup>

Using each of these assumptions to determine a gel's modulus with an AFM introduces some variability; however, AFM measurements of gel and cell modulus have been made repeatedly and successfully on multiple gels and cell types and have been part of several seminal works. For example, researchers have used AFM to characterize comprehensively the modulus of soft tissues and mimetic gels for studying mechanotransduction.<sup>[40,83,90]</sup> In addition, the interplay between substrate modulus and cell cytoskeletal organization and modulus has been investigated (Figure 7B).<sup>[89]</sup> With this tool, local modulus and crosslinking density are determined on surfaces and their influence on cell function probed, but it is still difficult to measure local modulus *within* a gel during 3D cell culture. Towards measuring and monitoring gel modulus and crosslinking density in 3D, microrheology is being explored.

## 8. Tracer Particle Microrheology

Microrheology utilizes the motion of micrometer-sized probe particles to determine the mechanical properties of the surrounding medium (Figure 8). Unlike AFM, which probes the material at the surface, microrheology allows access throughout the hydrogel volume. The probe particle motion is either actively manipulated via an external force, such as a magnetic field or light tweezers, or passively observed as they undergo Brownian motion. In either case, the probe particle motion is affected by the surrounding medium. Thus, by resolving the particle motion, one can access the local viscoelastic properties of the material.

To probe gel properties, tracer particle microrheology involves the encapsulation of small particles within hydrogel systems and following their motion in situ with light microscopy. This particle motion is subsequently correlated with local gel modulus and crosslinking density through a mathematical analysis of the forces acting on the sphere. The mathematical basis for tracer microrheology is the so-called generalized Langevin Equation, or particle force balance, which describes the driving force balanced by a material-based retardation force. The history dependent material properties of the surrounding medium are captured in the retardation force through a memory kernel, or history dependent friction coefficient normalized by the mass of the particle,  $\zeta_m$  (the second term on the right hand side of Equation 1).<sup>[91,92]</sup> As this form is analogous to the development of typical linear viscoelastic functions, such as the creep compliance or relaxation modulus, it is not surprising that this derivation provides a mathematical

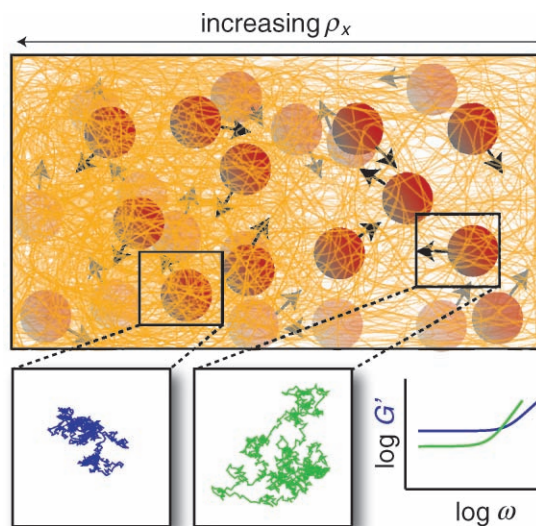


**Figure 8. Illustration of passive tracer microrheology in a hydrogel with a crosslinking density gradient.** The embedded probe particles (red spheres) undergo Brownian motion, whose path is characteristic of the surrounding hydrogel (yellow chains). The insets show typical paths for probe particles in a hydrogel having a gradient crosslinking density. With increasing crosslinking density, there is a decrease in the mean squared displacement of individual particles. After multiple particles have been observed, the ensemble-averaged viscoelastic properties are obtained.

framework to interpret the probe particle's spatial evolution (i.e., the momentum evolution,  $p(t)$ ) in terms of viscoelastic properties.

The solution of Equation 1 depends on the nature of the driving forces,  $F$ , which is either an external force or a stochastic Brownian force or the sum of both.

$$\frac{d p(t)}{d t} = \underline{F} - \int_{-\infty}^t d \tau \zeta_m(t - \tau) \underline{p}(\tau) \quad (1)$$

Passive tracer microrheology has a rich historical background that can be traced back to the work of Jean Perrin and a team of students who performed impressively precise position evolution measurements on colloidal particles undergoing Brownian motion, demonstrating the accuracy of the Stokes–Einstein relationship ( $\langle \Delta r^2(t) \rangle = k_B T / \pi a \eta$ , where  $\langle \Delta r^2(t) \rangle$  is the mean-squared displacement of a spherical particle having a radius  $a$  in a fluid with viscosity  $\eta$ ).<sup>[93]</sup> More recently, the Brownian motion of a spherical particle in viscoelastic materials was shown to follow the generalized Stokes–Einstein relationship, or GSER ( $\langle \Delta \tilde{r}^2(s) \rangle = k_B T / \pi a \tilde{\eta}(s)$ ),<sup>[94–96]</sup> where the mean-squared displacement is now a complex function expressed here in the Laplace domain,  $s$ ; this result is the solution of Equation 1, where  $F$  is a stochastic Brownian force.<sup>[96–98]</sup> The complex viscosity is conveniently transformed to the creep compliance in the time domain as  $J(t) = \langle \Delta r^2(t) \rangle \pi a / k_B T$ .<sup>[67,99]</sup> This last expression is used as a design equation to approximate the experimental particle displacement resolution and particle size needed to evaluate the elastic modulus of a material ( $G \leq 1/J$ ).<sup>[67]</sup> For example, an experimental particle displacement resolution of 10 nm (as obtained via video particle tracking<sup>[100]</sup>) for 500 nm size particles will have an upper modulus limit of  $\sim 0.05$  kPa. Thus, to measure the modulus of a covalently crosslinked hydrogel (0.1–100 kPa), the experimental resolution must be increased or the particle size must be reduced.

In the development of GSER via Equation 1, it is inherently assumed that the surrounding medium can be treated as a continuum; however, as the size-scale of the probe particle approaches the characteristic length-scale of the material (e.g., the mesh size of the hydrogel) GSER is expected to fail. Furthermore, probe particles may interact with and possibly influence their surrounding environment, affecting the viscoelastic measurements.<sup>[101–103]</sup> The probe particle interaction with the surrounding material can influence the viscoelastic property measurement by attraction or depletion effects, thereby enhancing or reducing the local concentration, respectively. Two-point tracer microrheology addresses this issue by utilizing particle–particle cross-correlations, which provide viscoelastic measurement of the material between the two particles.<sup>[104]</sup> Similar to how the two conductive spheres interact through a dielectric medium, two spheres undergoing Brownian motion exhibit correlations via a displacement field in a viscoelastic medium.<sup>[105,106]</sup>

Despite its limitations, passive tracer microrheology has been utilized in exploring the dynamics of multiple biologically relevant low modulus materials, such as F-actin.<sup>[107–109]</sup> The spatial evolution of dynamical properties in the cytoplasm of a live cell is achieved using multiple particle tracking of embedded probe particles.<sup>[54,110]</sup> Additionally, the formation of

hydrogels up to the gel-point has been examined using passive tracer microrheology,<sup>[111,112]</sup> which could similarly be used to characterize the degradation of a hydrogel undergoing a gel-to-sol transition. This characterization may prove rather beneficial for understanding the local process of matrix remodeling while a cell is migrating for quantitative analysis of cell-dictated degradation in complement to qualitative FRET-based assays.<sup>[59]</sup> In addition, this local, quantitative monitoring of degradation assists in establishing the critical matrix crosslinking densities for observing or dictating changes in cellular processes, such as spreading,<sup>[77]</sup> process extension,<sup>[113]</sup> and ECM elaboration and assembly.<sup>[114]</sup> A challenge remains in probing the mechanics of a covalently formed gel, whose modulus may be too high for the measurement resolution of passive microrheology until significant gel degradation has occurred. To address this limitation, active microrheology should be explored.

Active microrheological methods have the capability of producing larger displacements than passive methods, and therefore the displacements are easier to spatially resolve in materials possessing higher moduli. The application of an external force is readily incorporated into the generalized Langevin equation (Equation 1), where  $F$  becomes the sum of the Brownian and external forces. The two predominate methods used to exert an external force on a particle have produced forces through either an optical trap (laser tweezers)<sup>[115,116]</sup> or a magnetic tweezers (via current through a coil).<sup>[117]</sup> The optical trap method uses focused light to create a potential well, essentially trapping a spherical particle. The force on the particle depends on several factors, but is typically larger than that produced by Brownian motion. Unfortunately, this force is still too small to resolve the modulus for a majority of PEG-based hydrogels used in 3D culture. Furthermore, the hydrogel heterogeneity complicates laser-based microrheological methods, which need direct access to the probe particle. The recent use of powerful and precise magnetic fields produces forces on spherical magnetic particles up to many orders of magnitude greater than optical trapping techniques; however, these lack independent control of each particle.

Although recently there have been several advancements in both passive and active methods of tracer particle microrheology, their use to probe a 3D heterogeneous cellular scaffolds remains limited. The theoretical framework appears to be well developed, but there are several experimental factors that must be resolved. Passive methods, particularly two-point video particle tracking, have several advantages, such as obtaining property information both locally and between particles, but lack the resolution to examine the mechanical properties of fully formed, covalently crosslinked hydrogels. In order for passive tracer particle microrheology to be a viable option, new spatial tracking methods must be developed. Active methods exert an external force producing enhanced particle displacement and thus may be the most promising avenue to explore the hydrogel microenvironment. Despite the low external forces produced by optical trapping, exploration of thin hydrogels with low crosslinking density may be possible. This outcome would further allow individual cross-correlated motion to be explored, providing information on how mechanical disturbances are translated through the hydrogel matrix. Finally, magnetic fields that produce a large external force on magnetic particles may

be the simplest approach for exploring the hydrogel modulus. This method could provide information on the local heterogeneity of the material, as well as anisotropic effects that may be present in a 3D cell culture microenvironment.

## 9. Conclusions

This is an opportunistic time for advancements in cell-responsive hydrogel development and related characterization techniques. With the combination of advances in gel chemistries and techniques for monitoring the mechanics of cells and gels, questions about the complex interrelationships between microenvironment structure and cell function are being elucidated. Real-time monitoring techniques for detecting changes in cell function, such as gene expression, protein secretion, and migration, are routinely used, and complementary techniques to monitor related changes in the material environment surrounding cells are emerging, such as FRET-based assays to qualitatively characterize degradation of gels by encapsulated cells. For quantification of gel property changes, rheometry is being utilized to understand modification of bulk gel properties with crosslinking density and degradation. Local surface property effects on cell cytoskeletal organization are being probed with AFM, and microrheology is being employed to observe gel formation and cell mechanics in 3D and, with advances in measurement resolution through active tracer techniques, may be exploited to observe local gel degradation in the future. Through these approaches, the collection of methods for measuring changes in cell and gel properties is growing towards a better understanding of the dynamic relationship between a cell and its microenvironment.

## Acknowledgements

The authors would like to thank Mark W. Tibbitt for assistance with preparing some of the figures for this manuscript. The authors gratefully acknowledge the NIH (DE016523) and HHMI for funding.

Received: December 6, 2009

Published online: May 14, 2010

- [1] K. L. Schmeichel, M. J. Bissell, *J. Cell Sci.* **2003**, *116*, 2377.  
 [2] K. Ghosh, D. E. Ingber, *Adv. Drug Deliv. Rev.* **2007**, *59*, 1306.  
 [3] C. Adeloew, T. Segura, J. A. Hubbell, P. Frey, *Biomaterials* **2008**, *29*, 314.  
 [4] G. A. Silva, C. Czeisler, K. L. Niece, E. Beniash, D. A. Harrington, J. A. Kessler, S. I. Stupp, *Science* **2004**, *303*, 1352.  
 [5] R. M. Capito, H. S. Azevedo, Y. S. Velichko, A. Mata, S. I. Stupp, *Science* **2008**, *319*, 1812.  
 [6] S. C. Heilshorn, K. A. DiZio, E. R. Welsh, D. A. Tirrell, *Biomaterials* **2003**, *24*, 4245.  
 [7] S. A. Maskarinec, D. A. Tirrell, *Curr. Opin. Biotechnol.* **2005**, *16*, 422.  
 [8] B. V. Slaughter, S. S. Khurshid, O. Z. Fisher, A. Khademhosseini, N. A. Peppas, *Adv. Mater.* **2009**, *21*, 3307.  
 [9] S. Q. Liu, R. Tay, M. Khan, P. L. R. Ee, J. L. Hedrick, Y. Y. Yang, *Soft Matter* **2010**, *6*, 67.  
 [10] Z. J. Sui, W. J. King, W. L. Murphy, *Adv. Funct. Mater.* **2008**, *18*, 1824.  
 [11] S. J. Bryant, C. R. Nuttelman, K. S. Anseth, *J. Biomater. Sci.-Polym. Ed.* **2000**, *11*, 439.  
 [12] M. S. Hahn, J. S. Miller, J. L. West, *Adv. Mater.* **2006**, *18*, 2679.  
 [13] S. Lin-Gibson, R. L. Jones, N. R. Washburn, F. Horkay, *Macromolecules* **2005**, *38*, 2897.  
 [14] P. J. Flory, J. Rehner, *J. Chem. Phys.* **1943**, *11*, 512.  
 [15] N. S. Hwang, S. Varghese, Z. Zhang, J. Elisseeff, *Tissue Eng.* **2006**, *12*, 2695.  
 [16] M. P. Lutolf, J. A. Hubbell, *Biomacromolecules* **2003**, *4*, 713.  
 [17] A. Metters, J. Hubbell, *Biomacromolecules* **2005**, *6*, 290.  
 [18] B. D. Fairbanks, M. P. Schwartz, A. E. Halevi, C. R. Nuttelman, C. N. Bowman, K. S. Anseth, *Adv. Mater.* **2009**, *21*, 5005.  
 [19] C. A. DeForest, B. D. Polizzotti, K. S. Anseth, *Nat. Mater.* **2009**, *8*, 659.  
 [20] M. P. Lutolf, J. A. Hubbell, *Nat. Biotechnol.* **2005**, *23*, 47.  
 [21] G. P. Raeber, M. P. Lutolf, J. A. Hubbell, *Biophys. J.* **2005**, *89*, 1374.  
 [22] G. A. Hudalla, T. S. Eng, W. L. Murphy, *Biomacromolecules* **2008**, *9*, 842.  
 [23] S. H. Lee, J. J. Moon, J. L. West, *Biomaterials* **2008**, *29*, 2962.  
 [24] C. G. Williams, T. K. Kim, A. Taboas, A. Malik, P. Manson, J. Elisseeff, *Tissue Eng.* **2003**, *9*, 679.  
 [25] R. Derda, A. Laromaine, A. Mammoto, S. K. Y. Tang, T. Mammoto, D. E. Ingber, G. M. Whitesides, *Proc. Natl. Acad. Sci. USA* **2009**, *106*, 18463.  
 [26] C. Chung, M. Beecham, R. L. Mauck, J. A. Burdick, *Biomaterials* **2009**, *30*, 4287.  
 [27] K. Wolf, P. Friedl, *Clin. Exp. Metastasis* **2009**, *26*, 289.  
 [28] C. M. Ghajar, V. Suresh, S. R. Peyton, C. B. Raub, F. L. Meyskens, S. C. George, A. J. Putnam, *Mol. Cancer Ther.* **2007**, *6*, 552.  
 [29] M. P. Lutolf, G. P. Raeber, A. H. Zisch, N. Tirelli, J. A. Hubbell, *Adv. Mater.* **2003**, *15*, 888.  
 [30] Z. S. Patel, A. G. Mikos, *J. Biomater. Sci.-Polym. Ed.* **2004**, *15*, 701.  
 [31] G. P. Raeber, M. P. Lutolf, J. A. Hubbell, *Acta Biomater.* **2007**, *3*, 615.  
 [32] C. M. Nelson, M. M. VanDuijn, J. L. Inman, D. A. Fletcher, M. J. Bissell, *Science* **2006**, *314*, 298.  
 [33] I. M. Chung, N. O. Enemchukwu, S. D. Khaja, N. Murthy, A. Mantalaris, A. J. Garcia, *Biomaterials* **2008**, *29*, 2637.  
 [34] B. K. Mann, A. S. Gobin, A. T. Tsai, R. H. Schmedlen, J. L. West, *Biomaterials* **2001**, *22*, 3045.  
 [35] A. A. Aimetti, A. J. Machen, K. S. Anseth, *Biomaterials* **2009**, *30*, 6048.  
 [36] A. A. Aimetti, M. W. Tibbitt, K. S. Anseth, *Biomacromolecules* **2009**, *10*, 1484.  
 [37] H. Nagase, G. B. Fields, *Biopolymers* **1996**, *40*, 399.  
 [38] M. P. Lutolf, J. L. Lauer-Fields, H. G. Schmoekel, A. T. Metters, F. E. Weber, G. B. Fields, J. A. Hubbell, *Proc. Natl. Acad. Sci. USA* **2003**, *100*, 5413.  
 [39] D. E. Ingber, *Prog. Biophys. Mol. Biol.* **2008**, *97*, 163.  
 [40] A. J. Engler, S. Sen, H. L. Sweeney, D. E. Discher, *Cell* **2006**, *126*, 677.  
 [41] A. J. Engler, H. L. Sweeney, D. E. Discher, *Biophys. J.* **2005**, *88*, 500A.  
 [42] C. S. Chen, M. Mrksich, S. Huang, G. M. Whitesides, D. E. Ingber, *Science* **1997**, *276*, 1425.  
 [43] R. Singhi, A. Kumar, G. P. Lopez, G. N. Stephanopoulos, D. I. C. Wang, G. M. Whitesides, D. E. Ingber, *Science* **1994**, *264*, 696.  
 [44] A. Mammoto, D. E. Ingber, *Curr. Opin. Cell Biol.* **2009**, *21*, 864.  
 [45] A. Mammoto, S. Huang, K. Moore, P. Oh, D. E. Ingber, *J. Biol. Chem.* **2004**, *279*, 26323.  
 [46] S. J. Bryant, K. S. Anseth, D. A. Lee, D. L. Bader, *J. Orthop. Res.* **2004**, *22*, 1143.  
 [47] F. Chowdhury, S. Na, D. Li, Y. C. Poh, T. S. Tanaka, F. Wang, N. Wang, *Nat. Mater.* **2010**, *9*, 82.  
 [48] M. T. Frey, Y. L. Wang, *Soft Matter* **2009**, *5*, 1918.

- [49] B. N. G. Giepmans, S. R. Adams, M. H. Ellisman, R. Y. Tsien, *Science* **2006**, 312, 217.
- [50] S. B. VanEngelenburg, A. E. Palmer, *Curr. Opin. Chem. Biol.* **2008**, 12, 60.
- [51] O. Destaing, F. Saltel, P. Jurdic, F. A. Bard, *Mol. Biol. Cell* **2001**, 12, 1621.
- [52] J. Zhang, R. E. Campbell, A. Y. Ting, R. Y. Tsien, *Nat. Rev. Mol. Cell Biol.* **2002**, 3, 906.
- [53] K. Wolf, Y. I. Wu, Y. Liu, J. Geiger, E. Tam, C. Overall, M. S. Stack, P. Friedl, *Nat. Cell Biol.* **2007**, 9, 893.
- [54] D. Wirtz, *Ann. Rev. Biophys.* **2009**, 38, 301.
- [55] E. L. Baker, R. T. Bonnecaze, M. H. Zamao, *Biophys. J.* **2009**, 97, 1013.
- [56] S. A. Maskarinec, C. Franck, D. A. Tirrell, G. Ravichandran, *Proc. Natl. Acad. Sci. USA* **2009**, 106, 22108.
- [57] C. A. Reinhart-King, M. Dembo, D. A. Hammer, *Biophys. J.* **2008**, 95, 6044.
- [58] S. Sen, S. Kumar, *J. Biomech.* **2010**, 43, 45.
- [59] S. H. Lee, J. J. Moon, J. S. Miller, J. L. West, *Biomaterials* **2007**, 28, 3163.
- [60] H. J. Kong, C. J. Kim, N. Huebsch, D. Weitz, D. J. Mooney, *J. Am. Chem. Soc.* **2007**, 129, 4518.
- [61] L. R. G. Treloar, *Trans. Faraday Soc.* **1943**, 39, 0241.
- [62] L. R. G. Treloar, *Trans. Faraday Soc.* **1943**, 39, 0036.
- [63] H. M. James, E. Guth, *J. Chem. Phys.* **1943**, 11, 455.
- [64] F. T. Wall, *J. Chem. Phys.* **1942**, 10, 485.
- [65] P. G. de Gennes, *Scaling Concepts in Polymer Physics*, Cornell University Press, Ithaca, NY **1979**.
- [66] M. Rubinstein, R. H. Colby, *Polymer Physics*, Oxford University Press, New York **2003**.
- [67] J. D. Ferry, *Viscoelastic Properties of Polymers*, Wiley, New York **1980**.
- [68] F. Chambon, H. H. Winter, *Polym. Bull.* **1985**, 13, 499.
- [69] H. H. Winter, F. Chambon, *J. Rheol.* **1986**, 30, 367.
- [70] H. H. Winter, *Polym. Eng. Sci.* **1987**, 27, 1698.
- [71] R. J. Pelham, Y. L. Wang, *Proc. Natl. Acad. Sci. USA* **1997**, 94, 13661.
- [72] N. Zaari, P. Rajagopalan, S. K. Kim, A. J. Engler, J. Y. Wong, *Adv. Mater.* **2004**, 16, 2133.
- [73] S. R. Peyton, C. B. Raub, V. P. Keschrumrus, A. J. Putnam, *Biomaterials* **2006**, 27, 4881.
- [74] C. S. Chen, *J. Cell Sci.* **2008**, 121, 3285.
- [75] J. A. Burdick, A. Khademhosseini, R. Langer, *Langmuir* **2004**, 20, 5153.
- [76] K. Ghosh, C. K. Thodeti, A. C. Dudley, A. Mammoto, M. Klagsbrun, D. E. Ingber, *Proc. Natl. Acad. Sci. USA* **2008**, 105, 11305.
- [77] S. Khetan, J. S. Katz, J. A. Burdick, *Soft Matter* **2009**, 5, 1601.
- [78] P. J. Nowatzki, C. Franck, S. A. Maskarinec, G. Ravichandran, D. A. Tirrell, *Macromolecules* **2008**, 41, 1839.
- [79] A. M. Kloxin, M. W. Tibbitt, A. M. Kasko, J. F. Fairbairn, K. S. Anseth, *Adv. Mater.* **2010**, 22, 61.
- [80] J. J. Tomasek, G. Gabbiani, B. Hinz, C. Chaponnier, R. A. Brown, *Nat. Rev. Mol. Cell Biol.* **2002**, 3, 349.
- [81] K. Saha, A. J. Keung, E. F. Irwin, Y. Li, L. Little, D. V. Schaffer, K. E. Healy, *Biophys. J.* **2008**, 95, 4426.
- [82] J. Y. Wong, A. Velasco, P. Rajagopalan, Q. Pham, *Langmuir* **2003**, 19, 1908.
- [83] F. Guilak, D. M. Cohen, B. T. Estes, J. M. Gimble, W. Liedtke, C. S. Chen, *Cell Stem Cell* **2009**, 5, 17.
- [84] M. T. Frey, A. Engler, D. E. Discher, J. Lee, Y. L. Wang, in *Cell Mechanics*, Vol. 83, Elsevier Academic Press Inc, San Diego, CA **2007**, 47.
- [85] J. Domke, M. Radmacher, *Langmuir* **1998**, 14, 3320.
- [86] A. J. Engler, L. Richert, J. Y. Wong, C. Picart, D. E. Discher, *Surf. Sci.* **2004**, 570, 142.
- [87] M. Wang, R. J. Hill, *Soft Matter* **2008**, 4, 1048.
- [88] S. J. Bryant, K. S. Anseth, in *Scaffolding in Tissue Engineering* (Eds: P. X. Ma, J. Elisseeff), Marcel Dekker, Inc., New York **2005**, 69.
- [89] K. L. Moffat, W. H. S. Sun, P. E. Pena, N. O. Chahine, S. B. Doty, G. A. Ateshian, C. T. Hung, H. H. Lu, *Proc. Natl. Acad. Sci. USA* **2008**, 105, 7947.
- [90] J. Solon, I. Levental, K. Sengupta, P. C. Georges, P. A. Janmey, *Biophys. J.* **2007**, 93, 4453.
- [91] R. Kubo, *Rep. Prog. Phys.* **1966**, 29, 255.
- [92] H. Mori, *Prog. Theor. Phys.* **1965**, 33, 423.
- [93] J. Perrin, *Ann. Chim. Phys.* **1909**, 18, 1.
- [94] G. P. Devault, J. A. McLennan, *Phys. Rev.* **1965**, 137, A725.
- [95] R. Zwanzig, M. Bixon, *Phys. Rev. A* **1970**, 2, 2005.
- [96] T. G. Mason, D. A. Weitz, *Phys. Rev. Lett.* **1995**, 74, 1250.
- [97] C. Oelschlaeger, A. Schopferer, F. Scheffold, N. Willenbacher, *Langmuir* **2009**, 25, 716.
- [98] A. Palmer, T. G. Mason, J. Y. Xu, S. C. Kuo, D. Wirtz, *Biophys. J.* **1999**, 76, 1063.
- [99] J. Y. Xu, V. Viasnoff, D. Wirtz, *Rheol. Acta* **1998**, 37, 387.
- [100] J. C. Crocker, D. G. Grier, *J. Colloid Interface Sci.* **1996**, 179, 298.
- [101] M. T. Valentine, Z. E. Perlman, M. L. Gardel, J. H. Shin, P. Matsudaira, T. J. Mitchison, D. A. Weitz, *Biophys. J.* **2004**, 86, 4004.
- [102] B. S. Chae, E. M. Furst, *Langmuir* **2005**, 21, 3084.
- [103] A. S. B. Cucheval, R. R. Vincent, Y. Hemar, D. Otter, M. A. K. Williams, *Langmuir* **2009**, 25, 11827.
- [104] J. C. Crocker, M. T. Valentine, E. R. Weeks, T. Gisler, P. D. Kaplan, A. G. Yodh, D. A. Weitz, *Phys. Rev. Lett.* **2000**, 85, 888.
- [105] A. J. Levine, T. C. Lubensky, *Phys. Rev. E* **2002**, 65.
- [106] A. J. Levine, T. C. Lubensky, *Phys. Rev. Lett.* **2000**, 85, 1774.
- [107] F. C. Mackintosh, J. Kas, P. A. Janmey, *Phys. Rev. Lett.* **1995**, 75, 4425.
- [108] M. L. Gardel, M. T. Valentine, J. C. Crocker, A. R. Bausch, D. A. Weitz, *Phys. Rev. Lett.* **2003**, 91, 4.
- [109] T. Gisler, D. A. Weitz, *Phys. Rev. Lett.* **1999**, 82, 1606.
- [110] Y. Tseng, T. P. Kole, D. Wirtz, *Biophys. J.* **2002**, 83, 3162.
- [111] K. M. Schultz, A. D. Baldwin, K. L. Kiick, E. M. Furst, *Macromolecules* **2009**, 42, 5310.
- [112] K. M. Schultz, A. D. Baldwin, K. L. Kiick, E. M. Furst, *Soft Matter* **2009**, 5, 740.
- [113] M. J. Mahoney, K. S. Anseth, *Biomaterials* **2006**, 27, 2265.
- [114] J. L. Ifkovits, J. A. Burdick, *Tissue Eng.* **2007**, 13, 2369.
- [115] R. R. Brau, J. M. Ferrer, H. Lee, C. E. Castro, B. K. Tam, P. B. Tarsa, P. Matsudaira, M. C. Boyce, R. D. Kamm, M. J. Lang, *J. Opt. A-Pure Appl. Opt.* **2007**, 9, S103.
- [116] L. Starrs, P. Bartlett, *Faraday Discuss.* **2003**, 123, 323.
- [117] F. Amblard, B. Yurke, A. Pargellis, S. Leibler, *Rev. Sci. Instrum.* **1996**, 67, 818.